

Own Weight Effect on Static Analysis of Pre-Stretched Plate-Strip Containing Twin Circular Inclusions Under Bending

Ulku BABUSCU YESIL¹, Nazmiye YAHNIOGLU²

¹Yildiz Technical Uni., Faculty of Chemical and Metallurgical Eng., Dep. of Mathematical Engineering, Istanbul, Turkey

²Yildiz Technical Uni., Faculty of Chemical and Metallurgical Eng., Dep. of Mathematical Engineering, Istanbul, Turkey

*Corresponding author e-posta: ¹ubabescu@yildiz.edu.tr ORCID ID: <http://orcid.org/0000-0002-8557-8308>

²nazmiye@yildiz.edu.tr ORCID ID: <http://orcid.org/0000-0002-3921-8643>

Geliş Tarihi: 30.07.2018;

Kabul Tarihi: 25.11.2019

Abstract

This paper addresses the influence of own weight on the static analysis of the bending of a pre-stretched plate-strip containing twin round shaped inclusions made from the same materials and whose centers are on a line parallel to the free surface. The effects of body forces (own weight) and surface forces (pre-stretching load) on the plate-strip with inclusions are considered together as the initial stresses. The effects of these initial stresses on the analyses of stress concentration around the inclusions within a plate-strip under additional bending load are investigated by the Three-Dimensional Linearized Theory of Elasticity (TDLTE) under the plane strain state. Also, the solutions of the considered boundary value problems are worked out by using the Finite Elements Method. With respect to the results, it was revealed that the own weight of the plate-strip has a substantial influence on the static analysis around the circular twin inclusions within a plate-strip under bending.

Keywords

Own weight;
Circular inclusion;
Pre-stretched stress;
Static analysis;
Finite element method

Kendi Ağırlığının İkiz Dairesel Dolgular İçeren Eğilme Altındaki Öngerilmeli Şerit-Plağın Statik Analizine Etkisi

Öz

Bu çalışma, eğilme etkisi altında içerisinde aynı malzemeden yapılmış ve merkezleri serbest yüzeye paralel bir doğrultuda olan ikiz dairesel şekilli dolgular içeren öngerilmeli bir kompozit şerit-plağın statik analizine kendi ağırlığının etkisini ele almaktadır. Dolgular içeren şerit-plak üzerindeki hacimsel kuvvetlerin (kendi ağırlığı) ve yüzeysel kuvvetlerin (öngerilme yüklemesi) etkisi birlikte öngerilmeler olarak düşünülmüştür. Bu öngerilmelerinin, ek bir eğilme yükü altında bir şerit-plak içindeki dolgular etrafındaki gerilme dağılımlarının analizleri üzerindeki etkileri, düzlem şekil değiştirme durumu altında Lineerize Edilmiş Üç Boyutlu Elastisite Teorisi (LEÜBET) ile araştırılmaktadır. Ayrıca, ele alınan sınır değer problemlerinin çözümleri Sonlu Elemanlar Yöntemi kullanılarak gerçekleştirilmiştir. Sonuçlara göre, eğilme etkisi altındaki ikiz dairesel dolgular içeren şerit-plağın kendi ağırlığının plağın statik analizi üzerinde önemli bir etkisi olduğu ortaya çıkmıştır.

Anahtar kelimeler

Kendi ağırlığı;
Dairesel dolgu;
Öngerilme;
Statik analiz;
Sonlu elemanlar
metodu

© Afyon Kocatepe Üniversitesi

1. Introduction

Strength of structural elements are significantly affected by the existence of discontinuity, such as inclusions. The existence of inclusions in structural elements cause strain and stress concentration around these inclusions so mechanical characteristics of materials are affected

significantly. Eshelby studied the presence of ellipsoidal region in an infinite space by taking the elastic constants different from the rest of the material with the equivalent inclusion method (EIM) (Eshelby 1957). The influence of inclusions in structures were investigated widely by Christensen (1979), Mura (1988) and Mura et al. (1996) and Zhou

et al. (2013) and others. Dynamic analysis of pre-stretched plate containing circular shaped inclusions was studied by Babuscu Yesil (2015). However, own weight of the structures are neglected in these investigations, so heavyweight and lightweight structures were assumed as if equal. The own weight of the structures must not be ignored for ensuring the safe structural designs. The weight of structures is named as 'dead load'. Dead loads are modelled as static and permanent loads and play an important role in the collapse of structures (Takabatake 1990, 1991, 2012). If the contribution of own weights on the mechanics of structures is well appeared, getting more accurate results will be possible. Takabatake examined the influence of dead loads on closed-form estimation solution of the structures (Takabatake 1990, 1991, 2012). The stiffening consequence of the dead loads on mechanics of structures was studied for plates with the finite element method by Zhou (2002). In the above mentioned works the structures do not contain any discontinuity. Besides, there is a study which includes a hole in a plate-strip and investigate the influence of own weight on the stress distributions around this hole (Babuscu Yesil 2017). This paper aims to take into consideration the influence of own weight on the static analyses around twin circular inclusions with added bending forces on the upper surface of a pre-stretched plate-strip. During analysis process, Three-Dimensional Linearized Theory of Elasticity (TDLTE) is used for modelling the problem. In addition, Finite element method (FEM) is chosen for solving the problem. This is the first attempt to introduce the influence of own weight of the pre-stretched plate-strip containing twin circular shaped inclusions on static analysis.

2. Mathematical formulation

The influence of the own weight of the plate with initial forces comprising twin circular shaped inclusions on the stress and displacement distributions under bending are examined. Considering that the plate-strip's own weight and uniaxial stretching forces act together, there are two forces being applied on the plate in the

reference (initial) state. The distribution of stresses and strains of the plate-strip subjected to both initial forces are determined separately using the linear theory of elasticity, and then the superposition principle is applied for determination of their total effect.

The considered plate with twin circular inclusions is simply supported at $x_1=0$ and $x_1=\ell$ (Fig. 1). Besides, normal stretching forces which distributed uniformly and with intensity q acting $x_1=0$ and $x_1=\ell$ edges and body forces with intensity f acting the plate in the reference state. Furthermore, the plate is under bending forces with intensity p . For the solution methodology, the couple effect between body force and stretching force on the strain-stress distribution of the plate is not taken into account, but both the couple effect between each one and the additional force on the strain-stress distribution of the plate are taken into account.

The considered problem can be solved with two states: 1) the reference state and 2) the additional state. For the reference state, the displacement and stress distributions of the plate with twin circular inclusions are determined under body force and uniformly distributed uniaxial stretching force. These displacements (stresses) are named initial displacements (stresses). For the additional state, with considering the initial displacements and stresses obtained in the reference state, the displacement and stress distributions of the pre-stressed plate-strip with inclusions are obtained under bending forces which have uniform distributions.

In the following mathematical modelling of the problem, the quantities of the reference state will be indicated by the upper indices (0).

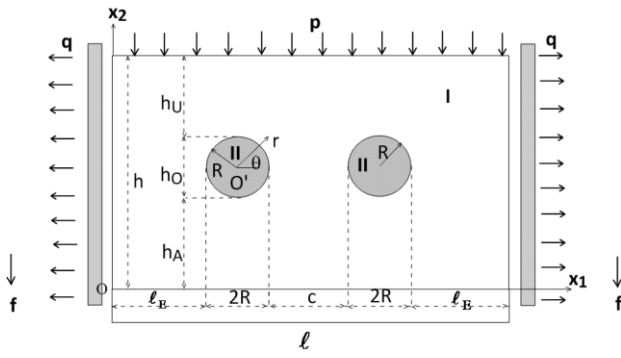


Figure 1. Coordinates and load distributions of the plate-strip with the same circular inclusions.

Solution domain of the boundary value problem is:

$$W = W \cup W_L \cup W_R = \{ 0 \leq x_1 \leq l, 0 \leq x_2 \leq h, -\infty \leq x_3 \leq \infty \}$$

$$W' = W / (W_L \cup W_R) \tag{1}$$

where

$$W_L = \left\{ (x_1, x_2) \mid (x_1 - (\ell_E + R))^2 + (x_2 - (h_A + R))^2 \leq R^2 \right\}$$

$$W_R = \left\{ (x_1, x_2) \mid (x_1 - (\ell - (\ell_E + R)))^2 + (x_2 - (h_A + R))^2 \leq R^2 \right\}$$

(2)

Reference state of the boundary value problem, which modelled in accordance with the linear theory of elasticity, given below.

$$\frac{\partial \sigma_{ij}^{(0),k}}{\partial x_j} + f_i = 0, \quad f_i = \rho g \delta_2^i$$

$$\sigma_{11}^{(0),k} = (\lambda_k + 2\mu_k) \varepsilon_{11}^{(0),k} + \lambda_k \varepsilon_{22}^{(0),k}$$

$$\sigma_{22}^{(0),k} = \lambda_k \varepsilon_{11}^{(0),k} + (\lambda_k + 2\mu_k) \varepsilon_{22}^{(0),k}$$

$$\sigma_{12}^{(0),k} = 2\mu_k \varepsilon_{12}^{(0),k}$$

$$\left(\lambda_k = \frac{\nu_k E_k}{(1 + \nu_k)(1 - 2\nu_k)}, \quad \mu_k = G_k = \frac{E_k}{2(1 + \nu_k)} \right)$$

$$\varepsilon_{ij}^{(0),k} = \frac{1}{2} \left(\frac{\partial u_i^{(0),k}}{\partial x_j} + \frac{\partial u_j^{(0),k}}{\partial x_i} \right), \quad i, j, k = 1, 2$$

$$u_2^{(0),1} \Big|_{x_1=0; \ell} = 0, \quad \sigma_{11}^{(0),1} \Big|_{x_1=0; \ell} = q \delta_1^i, \quad \sigma_{12}^{(0),1} \Big|_{x_1=0; \ell} = 0$$

$$\sigma_{12}^{(0),1} \Big|_{x_2=0; h} = 0, \quad u_i^{(0),1} \Big|_{I_L} = u_i^{(0),2} \Big|_{I_L}, \quad u_i^{(0),1} \Big|_{I_R} = u_i^{(0),2} \Big|_{I_R}$$

$$\sigma_{ji}^{(0),1} n_j \Big|_{I_L} = \sigma_{ji}^{(0),2} n_j \Big|_{I_L}, \quad \sigma_{ji}^{(0),1} n_j \Big|_{I_R} = \sigma_{ji}^{(0),2} n_j \Big|_{I_R} = 0 \tag{3}$$

Here

$$I_L = \left\{ (x_1, x_2) \mid (x_1 - (\ell_E + R))^2 + (x_2 - (h_A + R))^2 = R^2 \right\}$$

$$I_R = \left\{ (x_1, x_2) \mid (x_1 - (\ell - (\ell_E + R)))^2 + (x_2 - (h_A + R))^2 = R^2 \right\}$$

(4)

In Eq. (3) the superscript “k” denotes the corresponding values of the material of inclusions’ (matrix’s) for k=2 (k=1), f_i indicates the constituent of the density of the body force, g is the gravitational acceleration, ρ refers to the mass per unit volume of the analyzed plate material. I_R (I_L) denotes the contour of the right (left) inclusion.

The additional state of the boundary value problem which modelled by applying TDLTE, given below.

$$\frac{\partial}{\partial x_j} \left(\sigma_{ji}^k + \sigma_{it}^{(0),k} \frac{\partial u_i^k}{\partial x_t} \right) = 0$$

$$\sigma_{11}^k = (\lambda_k + 2\mu_k) \varepsilon_{11}^k + \lambda_k \varepsilon_{22}^k$$

$$\sigma_{22}^k = \lambda_k \varepsilon_{11}^k + (\lambda_k + 2\mu_k) \varepsilon_{22}^k$$

$$\sigma_{12}^k = 2\mu_k \varepsilon_{12}^k$$

$$\epsilon_{ij}^{:k} = \frac{1}{2} \left(\frac{\partial u_i^{:k}}{\partial x_j} + \frac{\partial u_j^{:k}}{\partial x_i} \right)$$

$$u_2^1 \Big|_{x_1=0;\ell} = 0, \left(\sigma_{jt}^1 + \sigma_{it}^{(0),1} \frac{\partial u_i^1}{\partial x_t} \right) n_j \Big|_{x_1=0;\ell} = 0$$

$$\left(\sigma_{ji}^1 + \sigma_{it}^{(0),1} \frac{\partial u_i^1}{\partial x_t} \right) n_j \Big|_{x_2=h} = p\delta_2^1, \left(\sigma_{ji}^1 + \sigma_{it}^{(0),1} \frac{\partial u_i^1}{\partial x_t} \right) n_j \Big|_{x_2=0} = 0$$

$$u_i^1 \Big|_{I_L} = u_i^2 \Big|_{I_L}, \quad u_i^1 \Big|_{I_R} = u_i^2 \Big|_{I_R}$$

$$\left(\sigma_{ji}^1 + \sigma_{it}^{(0),1} \frac{\partial u_i^1}{\partial x_t} \right) n_j \Big|_{I_L} = \left(\sigma_{ji}^2 + \sigma_{it}^{(0),2} \frac{\partial u_i^2}{\partial x_t} \right) n_j \Big|_{I_L} = 0$$

$$\left(\sigma_{ji}^1 + \sigma_{it}^{(0),1} \frac{\partial u_i^1}{\partial x_t} \right) n_j \Big|_{I_R} = \left(\sigma_{ji}^2 + \sigma_{it}^{(0),2} \frac{\partial u_i^2}{\partial x_t} \right) n_j \Big|_{I_R} = 0$$

$$i, j, t, k=1, 2 \tag{5}$$

For the considered boundary value problems in both stages, FEM modelling will be done using functionals and Ritz Technique (Akbarov 2013, Guz 1999, Guz 1999) For this purpose, for the FEM modelling of reference state (3) the functional

$$\begin{aligned} \Pi^{(0)} = & \frac{1}{2} \iint_{W'} \sigma_{ij}^{(0),1} \epsilon_{ij}^{(0),1} dx_1 dx_2 + \frac{1}{2} \iint_{W_L} \sigma_{ij}^{(0),2} \epsilon_{ij}^{(0),2} dx_1 dx_2 + \\ & \frac{1}{2} \iint_{W_R} \sigma_{ij}^{(0),2} \epsilon_{ij}^{(0),2} dx_1 dx_2 - \iint_W u_2^T f dx_1 dx_2 - \int_0^h q u_1^{(0),1} \Big|_{x_1=0} dx_2 + \\ & \int_0^h q u_1^{(0),1} \Big|_{x_1=\ell} dx_2 \end{aligned} \tag{6}$$

and for the FEM modelling of the additional state (5) the functional

$$\begin{aligned} \Pi = & \frac{1}{2} \iint_{W'} \left(T_{ij}^1 \frac{\partial u_j^1}{\partial x_i} \right) dx_1 dx_2 + \frac{1}{2} \iint_{W_L} \left(T_{ij}^2 \frac{\partial u_j^2}{\partial x_i} \right) dx_1 dx_2 + \\ & \frac{1}{2} \iint_{W_R} \left(T_{ij}^2 \frac{\partial u_j^2}{\partial x_i} \right) dx_1 dx_2 - \int_0^{\ell} p u_2^1 \Big|_{x_2=h} dx_1 \end{aligned} \tag{7}$$

are used, where

$$T_{ij}^{:k} = \sigma_{ij}^{:k} + \sigma_{it}^{(0),k} \frac{\partial u_i^{:k}}{\partial x_t}, \quad i, j, t, k = 1, 2 \tag{8}$$

In Eq. (8), $\sigma_{it}^{(0)}$ is the constituent of the initial stresses identified from the solution of the boundary value problem (3). The solution domain $W (= W' \cup W_L \cup W_R)$ is discretized a number of finite elements. For this purpose, curvilinear triangular shaped finite elements (FE) and rectangular shaped Lagrange family quadratic elements are used. (Zienkiewicz and Taylor 1989) (Figure 2a-2b).

W is divided by the finite elements as:

$$W = \bigcup_{k=1}^M W_k \tag{9}$$

here W_k represents the k-th finite element.

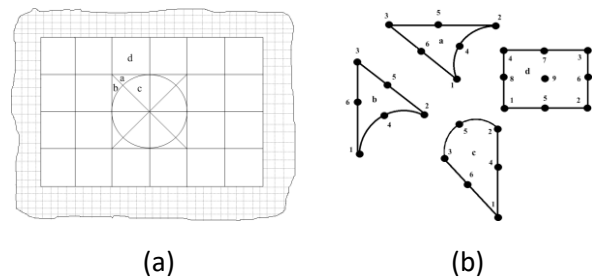


Figure 2. (a) Finite Element Mesh, (b) Finite elements with nodes.

For the rectangular finite elements, Standard Lagrange family shape functions are used. (Babuscu Yesil 2015, Zienkiewicz and Taylor 1989). However, for a triangular FE, the shape functions have the following form;

$$N_i = a + bx + cy + dx^2 + exy + fy^2 \tag{10}$$

and six coefficients are determined (Guz 2004),

$$N_j(x_{1k}, x_{2k}) = \delta_{jk}, \quad j, k = 1, 2, \dots, 6 \quad (11)$$

In Eq. (11) (x_{1k}, x_{2k}) denotes of the k-th node's abscissa and ordinate. For FEM modelling only displacements are considered as unknowns at the nodes, i.e. a displacement-based finite element formulation is used. So the displacement functions in the n-th FE have the form:

for the reference state (3)

$$\mathbf{u}^{(0),k,n} \approx \mathbf{N}^{k,n} \mathbf{a}^{(0),k,n}, \quad (12)$$

and for the additional state (5)

$$\mathbf{u}^{k,n} \approx \mathbf{N}^{k,n} \mathbf{a}^{k,n}, \quad (13)$$

where $k=1,2$ and $n=1,2,\dots,M$.

In Eqs. (12) and (13),

$$\left(\mathbf{a}^{(0),k,n} \right)^T = \left\{ u_{11}^{(0),k,n}, u_{21}^{(0),k,n}, \dots, u_{2s}^{(0),k,n}, u_{2s}^{(0),k,n} \right\} \quad (14)$$

$$\left(\mathbf{a}^{k,n} \right)^T = \left\{ u_{11}^{k,n}, u_{21}^{k,n}, \dots, u_{2s}^{k,n}, u_{2s}^{k,n} \right\} \quad (15)$$

$$\mathbf{N}^{k,n} = \begin{Bmatrix} N_1^{k,n} & 0 & \dots & N_s^{k,n} & 0 \\ 0 & N_1^{k,n} & \dots & 0 & N_s^{k,n} \end{Bmatrix} \quad n=1,2,\dots,M \quad (16)$$

In Eqs. (14) - (16), s is taken 6 (8) for a triangular (rectangular) finite element.

Finally substituting Eqs. (12) and (13) in the related functionals (6) and (7) respectively, corresponding algebraic equations systems are obtained as:

for the reference state,

$$\mathbf{K}^{(0)} \mathbf{a}^{(0)} = \mathbf{r}^{(0)} \quad (17)$$

and for the additional state,

$$\mathbf{K} \mathbf{a} = \mathbf{r} \quad (18)$$

Displacements at the nodes are obtained by solution to the algebraic equations given in Eq. (17) and Eq. (18). The additional state needs the values of the stresses obtained from the reference state, because Eq. (18) contains the stress values achieved

from the solution to the reference state. By solving the Eq. (17) and using the Hooke's Law they are achieved.

Design of the mesh and the selection of the elements are the same for both boundary value problems. Note that the numerical calculation of integrals is made with Gaussian Quadratures by using 10 points. Polar coordinate system $O'r\theta x_3$ (Fig. 1) around the circular inclusions are used (Babuscu Yesil 2015).

3. Numerical results

During all analysis, it is assumed that the inclusions and matrix are consisted of different materials and isotropic ones and ideal contact conditions in the interface surface are satisfied. The values of the matrix's materials are labelled by the subscript 1 and inclusions' materials are labelled by the subscript 2. The present study is investigated by assumption of plane strain state. The solution domain and loadings have symmetry with respect to $x_1 = \ell/2$, thus; only half of the solution domain is considered for the solution procedure. The solution domain is divided into 956 rectangular and 16 curvilinear triangular finite elements (Fig. 2). Hence, for the finite element modelling 4041 nodes and 8032 number degrees of freedoms are employed in total. For the validation of the present results, the numerical solutions of stresses are compared for four different test problems in the case where $E_2/E_1 = 1$.

Problem 1: Rectangular plate subjected to only plate's own weight (no external load),

Problem 2: Rectangular plate subjected to a uniform bending load (i.e., intensity of which compensate to the plate's own weight) acting on the top of the plate,

Problem 3: The modified case of Problem 2

The modified state is obtained by taking $p = \rho gh$ in Problem 1 and also by putting on the stresses $\sigma_{11} = 0$, $\sigma_{22} = \rho gy$, $\tau_{12} = 0$ (Timoshenko and Goodier 1970).

Problem 4: Exact solution for the plate-strip under bending without any defects (Timoshenko and Goodier 1970).

For the first three problems, the finite element analysis is used for solving the considered boundary value problems. Exact solution is given for the plate-strip under bending in Problem 4. The graphs in Figs. 3 and 4 exhibit the comparison on the stresses of σ_{11}/p and σ_{22}/p at $x_2=h$ for four problems. It follows from these graphs that the FEM solutions of the first three problems converge in appropriate cases to the exact solution of the 4th problem which is given in the Timoshenko and Goodier 1970, so the present work confirms the good agreement of the exact solution and finite element analysis.

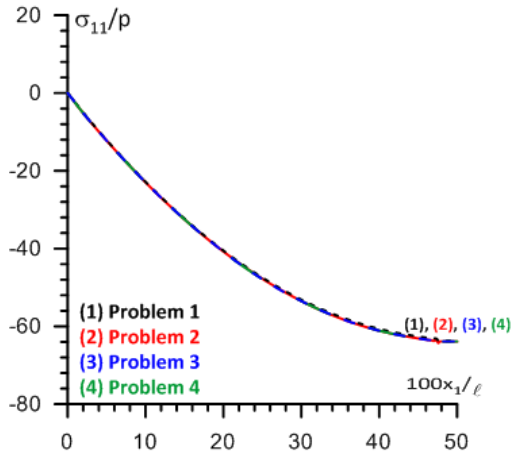


Figure 3. Comparison of the stresses of σ_{11}/p .

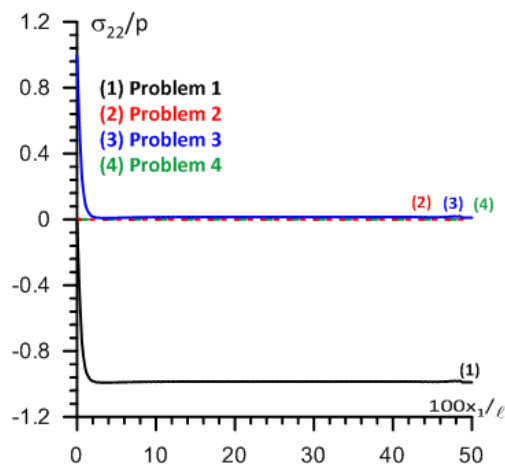
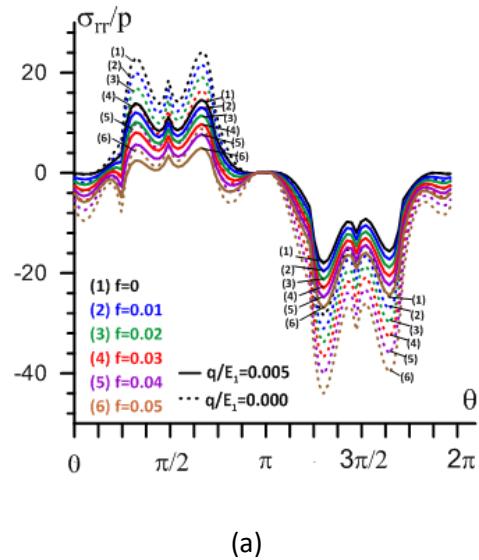


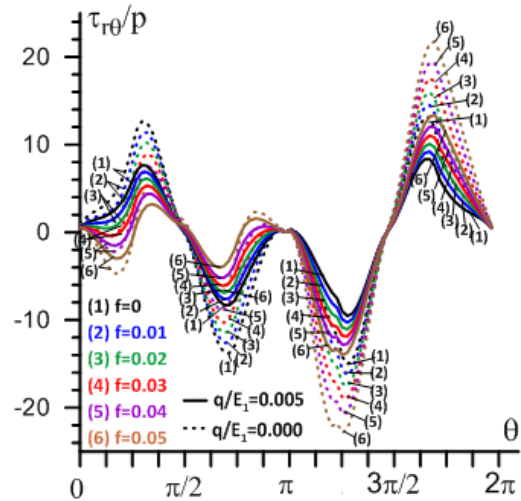
Figure 4. Comparison of the stresses of σ_{22}/p .

For the numerical results, it is assumed that Poisson coefficients $\nu^{(1)} = \nu^{(2)} = 0.3$, volume fractions $\eta^{(1)} = \eta^{(2)} = 0.5$, height of plate-strip $h/\ell = 0.10$, and radius of inclusions $R/\ell = 0.00833$, unless specified otherwise. Plotted in Fig. 5 (a, b, c) are the

polar stress distributions (a) σ_{rr}/p , (b) $\tau_{r\theta}/p$ and (c) $\sigma_{\theta\theta}/p$, respectively under various densities of own weight f , around the inclusions ($r=R$) for $E_2/E_1 = 5$, $h_U/R = 5$ with $q/E_1 = 0; 0.005$. It is established that the stresses $|\sigma_{\theta\theta}/p|$ become greater in amount with the density of own weight f , while the stresses $|\sigma_{rr}/p|$ and $|\tau_{r\theta}/p|$ decrease with the density of own weight. In these graphics the dotted curves represent the state $q/E_1 = 0$ and the solid curves represent $q/E_1 = 0.005$.



(a)



(b)

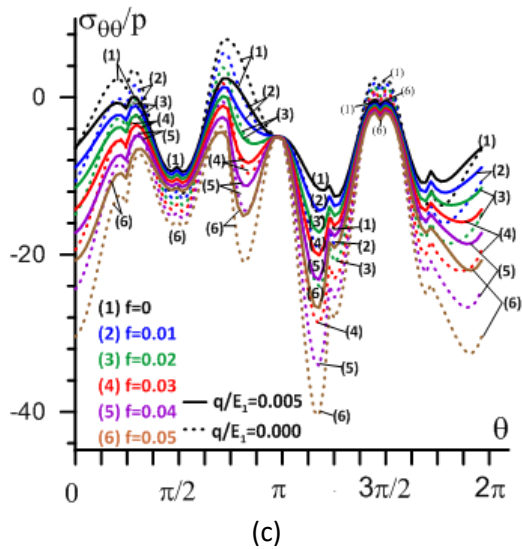


Figure 5. The stress distributions of (a) σ_{rr}/p , (b) $\tau_{r\theta}/p$, (c) $\sigma_{\theta\theta}/p$ around inclusions for various weight density (f) under $E_2/E_1 = 5$ for two cases of q/E_1 .

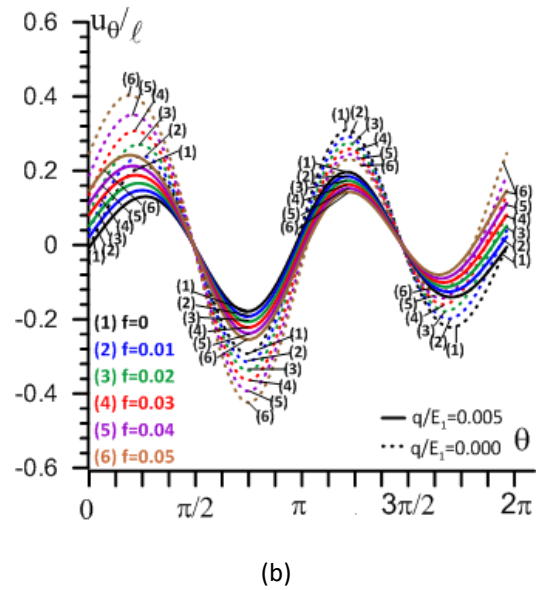
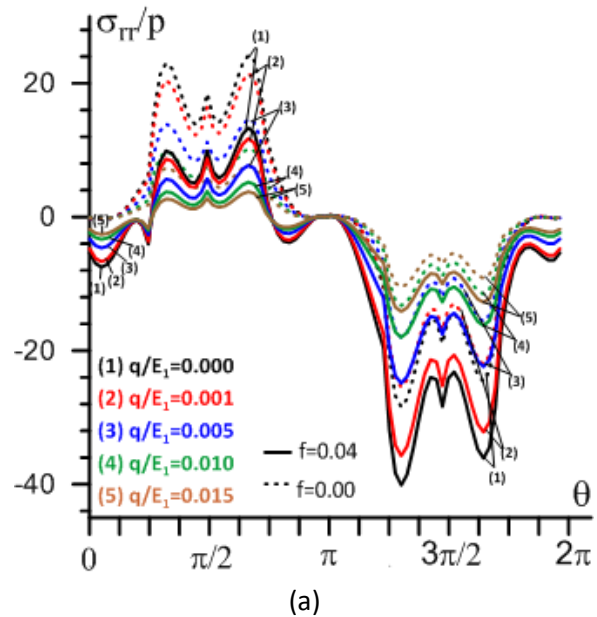
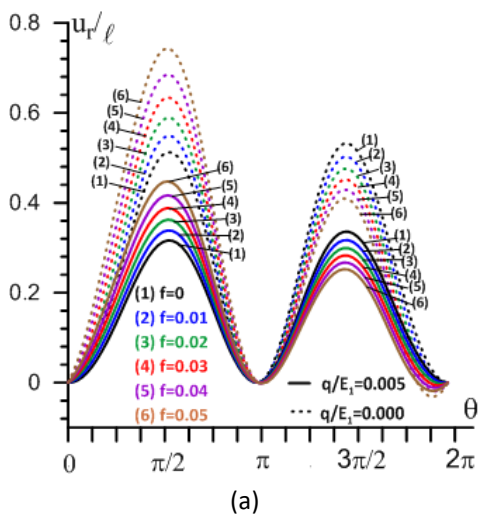
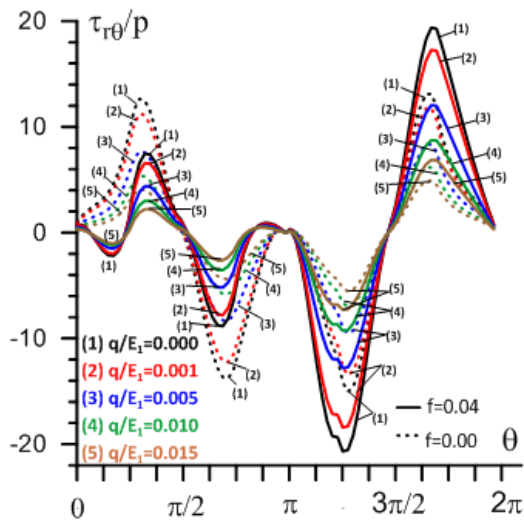


Figure 6. The displacement distribution of (a) u_r/l and (b) u_θ/l around the inclusions for various weight density (f) under $E_2/E_1 = 5$ for two cases of q/E_1 .

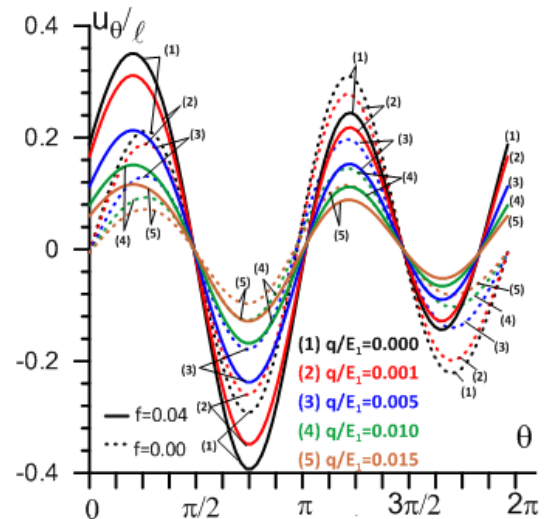
The influence of the density of own weight f on the values of the displacement distributions of (a) u_r/l and (b) u_θ/l , respectively, is given at $r=R$ under $E_2/E_1 = 5$ and $h_U/R = 5$ for $q/E_1 = 0$ (dotted line) and $q/E_1 = 0.005$ (solid line) in Fig. 6. The graphs show that the displacements $|u_r/l|$ and $|u_\theta/l|$ increase with the own weight at $\theta \in (0, \pi)$, but decrease at $\theta \in (\pi, 2\pi)$. The results for the displacements u_r/l and u_θ/l obtained in the initial stretching plate-strip i.e. $q/E_1 \neq 0$ are less than the corresponding values of these for $q/E_1 = 0$.

The effect of the initial force of q/E_1 on the stress distributions of (a) σ_{rr}/p , (b) $\tau_{r\theta}/p$ and (c) $\sigma_{\theta\theta}/p$, and displacement distributions of (d) u_r/l and (e) u_θ/l around the inclusions at $r=R$ under $E_2/E_1 = 5$ and $h_U/R = 5$ for $f = 0$ (dotted line) and $f = 0.04$ (solid line) are shown in Fig. 7. Absolute values of displacements and stresses decrease with q/E_1 for both $f = 0$ and $f \neq 0$.



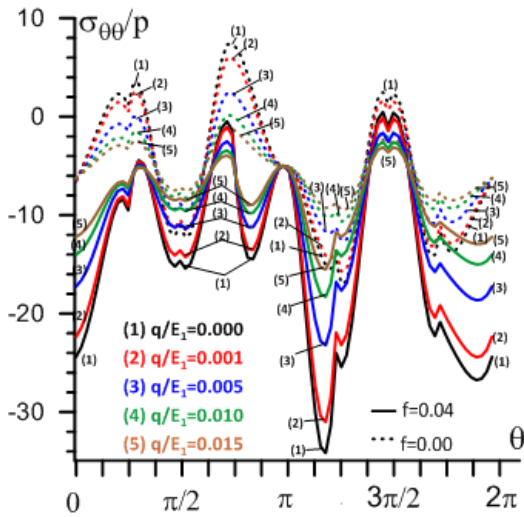


(b)

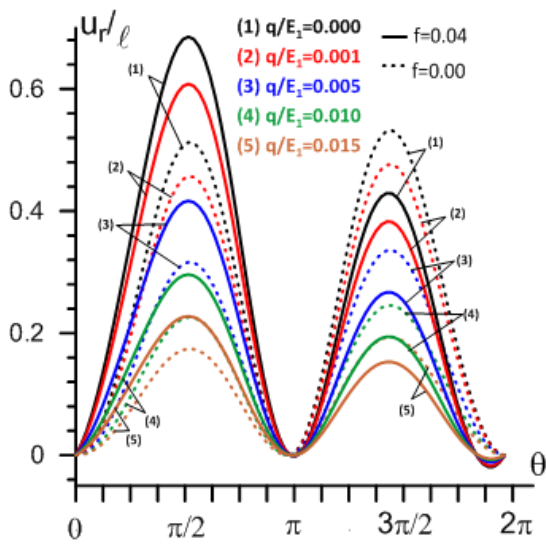


(e)

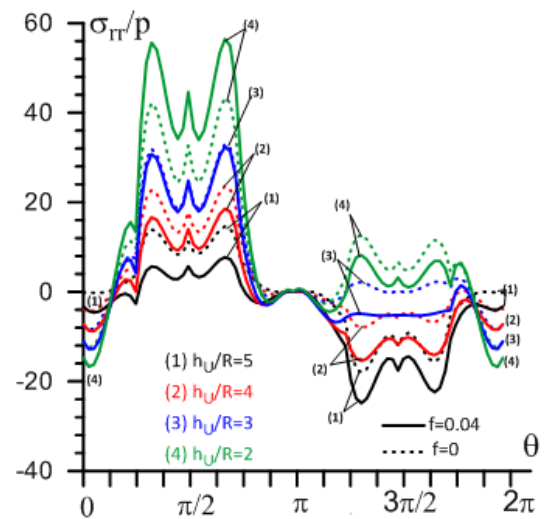
Figure 7. Stress distributions of (a) σ_{rr}/p , (b) $\tau_{r\theta}/p$, (c) $\sigma_{\theta\theta}/p$ and displacement distributions of (d) u_r/ℓ and (e) u_{θ}/ℓ around the inclusions for various q/E_1 under $E_2/E_1 = 5$, for $f = 0$ & $f = 0.04$.



(c)

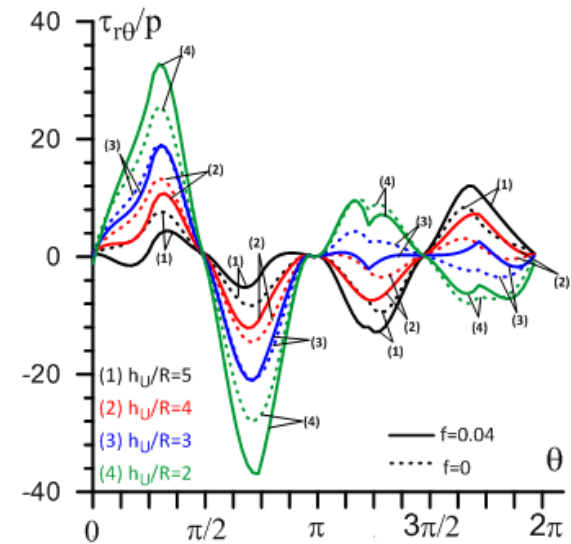


(d)

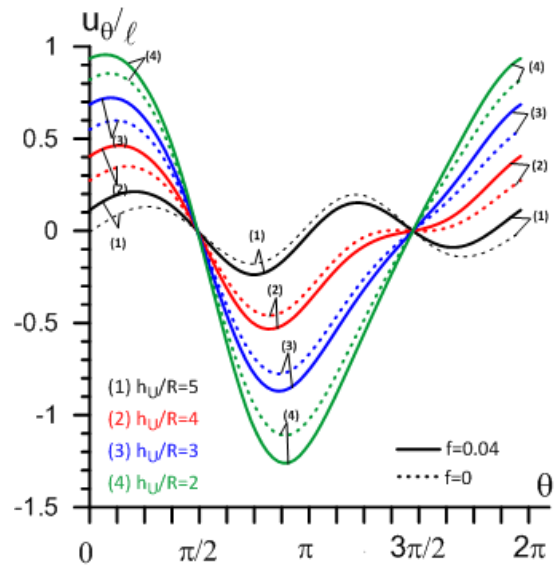


(a)

The effect of distance from the top of the inclusions to the upper face plane of the plate-strip i.e. h_U/R on the stress distributions of (a) σ_{rr}/p , (b) $\tau_{r\theta}/p$, (c) $\sigma_{\theta\theta}/p$ and displacement distributions of (d) u_r/ℓ and (e) u_{θ}/ℓ , around the inclusions at $r=R$ under $E_2/E_1 = 5$ and $q/E_1 = 0.005$ for cases $f = 0$ (dotted line) and $f = 0.04$ (solid line) are shown in Fig. 8. It is found that, the magnitudes of all stresses and displacements increase while h_U/R decrease for $f = 0$ and $f \neq 0$.

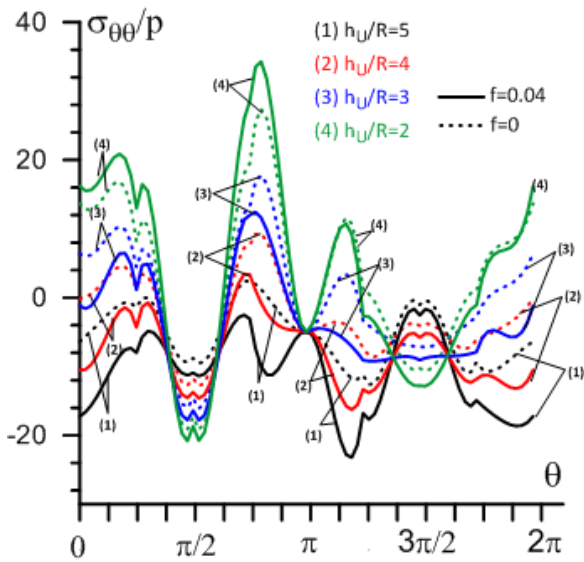


(b)

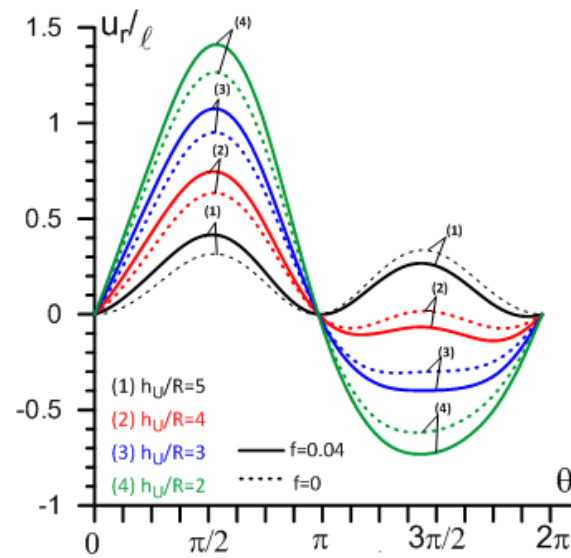


(e)

Figure 8. The stress distributions of (a) σ_{rr}/p , (b) $\tau_{r\theta}/p$, (c) $\sigma_{\theta\theta}/p$ and displacement distributions of (d) u_r/ℓ and (e) u_θ/ℓ around the inclusions for various h_U/R under $E_2/E_1 = 5$, and $q/E_1 = 0.005$ for $f = 0$ and $f = 0.04$.

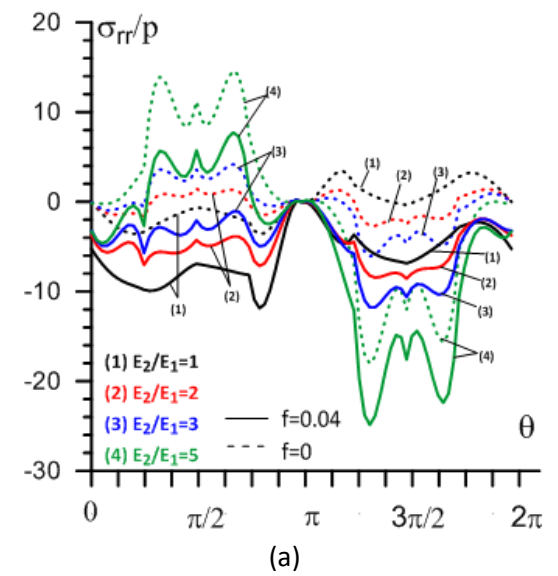


(c)

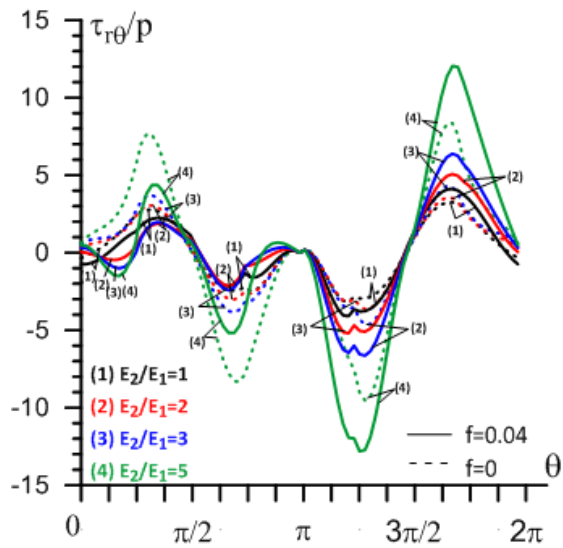


(d)

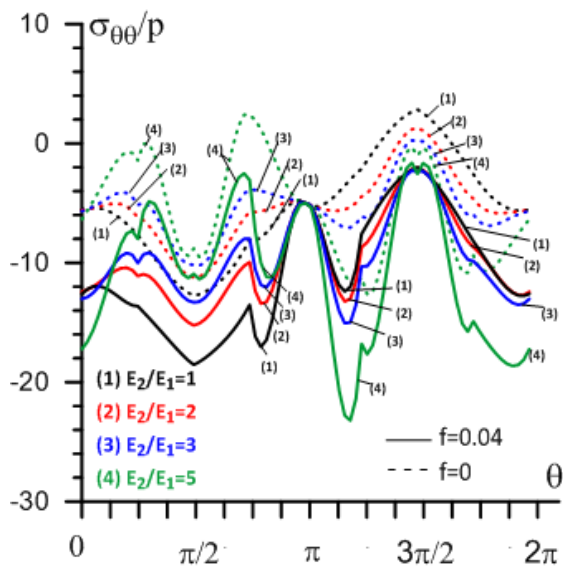
The effect of E_2/E_1 on the stress distributions of (a) σ_{rr}/p , (b) $\tau_{r\theta}/p$, (c) $\sigma_{\theta\theta}/p$ respectively, around the inclusions at $r=R$ under $q/E_1 = 0.005$ for $f = 0$ and $f = 0.04$ are shown in Fig. 9. All the magnitudes of stresses increase with E_2/E_1 for $f = 0$ and $f \neq 0$.



(a)



(b)



(c)

Figure 9. The stress distributions of (a) σ_{rr}/p , (b) $\tau_{r\theta}/p$, (c) $\sigma_{\theta\theta}/p$ around inclusions for various E_2/E_1 under $q/E_1 = 0.005$ for $f = 0$ and $f = 0.04$.

Table 1 illustrates the effect of E_2/E_1 , and distance among the two inclusions i.e. c/ℓ , on the stresses of $(\sigma_{\theta\theta}/p)|_{(f=0)}$ (numerator of the ratio) and $(\sigma_{\theta\theta}/p)|_{(f=0.04)}$ (denominator of the ratio) for $q/E_1 = 0.005$ at some points around the circular inclusions at $r=R$.

According to the given numerical values in Table 1, the stresses of $|\sigma_{\theta\theta}/p|$ increase with ratio of elasticity modulus (i.e. E_2/E_1) at the point $\theta = 0$

, but decrease at the points $\theta = \pi/4, \pi/2$ and $3\pi/4$ for both cases $f = 0$ and $f = 0.04$. The values of $\sigma_{\theta\theta}/p$ at the point $\theta = \pi$ do not change with the changes of the E_2/E_1 and c/ℓ values, so the values for this point have not been given in the table. With respect to the numerical results shown in Table 1, it is reveal that the stresses of $\sigma_{\theta\theta}/p$ for the selected points achieved for $f = 0.04$ are larger than the corresponding values achieved under $f = 0$.

Table 1. Influence of c/ℓ and E_2/E_1 on $(\sigma_{\theta\theta}/p)|_{(f=0)}$ (numerator of the ratio) and $(\sigma_{\theta\theta}/p)|_{(f=0.04)}$ (denominator of the ratio) at some points around the circular inclusions ($q/E_1 = 0.005$).

E_2/E_1	θ	c/ℓ						
		0.4709	0.2850	0.1487	0.0743	0.0247	0.0124	
1	0	-5.5579	-5.5545	-5.5507	-5.5481	-5.5462	-5.5464	
		-11.0575	-12.3083	-12.6586	-12.6096	-12.4830	-12.4468	
	$\pi/4$	-5.3861	-6.5790	-7.3012	-7.6483	-7.8631	-7.9149	
		-8.7902	-11.7730	-13.1753	-13.6387	-13.8387	-13.8749	
	$\pi/2$	-11.1123	-12.1833	-12.6350	-12.7675	-12.8118	-12.8174	
		-12.5267	-16.4169	-18.0957	-18.5479	-18.6940	-18.7124	
	$3\pi/4$	-9.3101	-8.7776	-8.3287	-8.0584	-7.8670	-7.8175	
		-10.3975	-12.3718	-13.2852	-13.5117	-13.5478	-13.5481	
	2	0	-5.6501	-5.6263	-5.6086	-5.5982	-5.5945	-5.5968
			-11.7436	-12.5305	-12.6146	-12.4317	-12.1866	-12.1301
		$\pi/4$	-5.1659	-5.7160	-6.0567	-6.2233	-6.3153	-6.3167
			-8.7180	-10.2890	-10.9482	-11.1102	-11.1451	-11.2084
$\pi/2$		-9.9609	-10.7947	-11.1410	-11.2398	-11.2813	-11.3064	
		-10.8233	-13.6590	-14.8992	-15.2466	-15.4344	-15.5166	
$3\pi/4$		-6.3963	-6.0783	-5.8552	-5.7343	-5.6537	-5.6330	
		-7.7505	-8.9427	-9.6776	-9.9487	-10.0352	-10.0579	
5		0	-6.3401	-6.3652	-6.3715	-6.3584	-6.3715	-6.4123
			-16.7361	-17.5226	-17.6257	-17.2357	-16.7906	-16.9951
		$\pi/4$	-2.4970	-1.8232	-1.5209	-1.4175	-1.4539	-1.5933
			-8.7452	-8.5766	-8.3237	-7.9981	-7.7569	-8.2056
	$\pi/2$	-8.0439	-8.5425	-8.7473	-8.8056	-8.8108	-8.7485	
		-8.4177	-10.0199	-10.7201	-10.9288	-11.1152	-11.1792	
	$3\pi/4$	0.7525	1.8339	2.2721	2.3949	2.3568	2.2039	
		-2.4912	-2.2408	-2.7645	-3.0772	-2.9807	-3.1355	

3. Conclusions

In this study, the own weight effect of the pre-stressed composite plate-strip with twin circular inclusions under bending on displacements and stress concentrations is numerically solved using the Finite Element Analysis in the framework of the TDLTE. The numerical outcomes point out the following conclusions:

- The influence of the plate-strip's own weight on the values of $|\sigma_{\theta\theta}/p|$ increase for $\theta \in (0, 2\pi)$, but $|\sigma_{rr}/p|$ and $|\tau_{r\theta}/p|$ ($|u_r/\ell|$ and $|u_\theta/p|$) decrease (increase) for $\theta \in (0, \pi)$, but increase (decrease) for $\theta \in (\pi, 2\pi)$ around the inclusions,

- The pre-stretching forces lead a decrease in the values of $|\sigma_{\theta\theta}/p|$, $|\sigma_{rr}/p|$, $|\tau_{r\theta}/p|$, $|u_r/\ell|$ and $|u_\theta/p|$,
- The differences between the displacements and stresses obtained at $f = 0$ and $f = 0.04$ decrease with q/E_1 ,
- The magnitudes of the displacements and stresses increase with decreasing the height between the top of the inclusions and the upper surface of the plate-strip i.e. h_U/R ,
- The absolute values of the stresses increase with E_2/E_1 .

According to all the conclusions given above, the own weight of a structure with inclusions cannot be

ignored for analyzing the deformation of solid mechanics.

Acknowledgment

We would like to show our gratitude to the Prof. Dr. Surkhay D. AKBAROV for his guidance and advice.

References

- Akbarov S.D., 2013. Stability Loss and Buckling Delamination: Three-Dimensional Linearized Approach for Elastic and Viscoelastic Composites, Springer-Heidelberg, New York, 71-132.
- Babuscu Yesil U., 2015. Forced Vibration Analysis of Prestretched Plates With Twin Circular Inclusions. *Journal of Engineering Mechanics*, **141 (1)**, 04014099-1-04014099-16.
- Babuscu Yesil U., 2017. The Effect of Own Weight On The Static Analysis of A Pre-stretched Plate-Strip With A Circular Hole In Bending. *Mechanics of Composite Materials*, **53(2)**, 243-252.
- Christensen, R.M., 1979. *Mechanics of Composite Materials*, Wiley, New York, 1-30.
- Eshelby, J.D., 1957. The determination of the elastic field of an ellipsoidal inclusion and related problems. *Proceeding of the Royal Society of London. Series A. Mathematical and Physical Sciences*, **241**, 376-396.
- Guz A.N., 1999. *Fundamentals of the Three-Dimensional Theory of Stability of Deformable Bodies*, Springer-Verlag, Berlin, 85-98.
- Guz A.N., 2004. *Elastic Waves in Bodies with Initial (Residual) Stresses [in Russian]*, Kiev, 102-136.
- Mura, T., 1988. Inclusion Problems. *Applied Mechanics Reviews*, **41**, 15-20.
- Mura, T., Shodja, H.M. and Hirose, Y., 1996. Inclusion Problems. *Applied Mechanics Reviews*, **49**, 118-127.
- Takabatake H., 1990. Effects of dead loads in static beams. *Journal of Structural Engineering-ASCE*, **116 (4)**, 1102-1120.
- Takabatake H., 1991. Static analyses of elastic plates with voids. *International Journal of Solids and Structures*, **28 (2)**, 179-196.
- Takabatake H., 2012. Effects of dead loads on the static analysis of plates. *Structural Engineering and Mechanics*, **42 (6)**, 761-781.
- Timoshenko S. P. and Goodier J. N., 1970, *Theory of Elasticity*, Third Edition, McGraw-Hill International Editions, London, 29-53.
- Zhou S. J., 2002. Load-induced stiffness matrix of plates. *Canadian Journal of Civil Engineering*, **29 (1)**, 181-184.
- Zhou, K., Hoh, H.J., Wang, X., Keer, L.M., Pang, J.H.L., Song, B. and Wang, Q.J., 2013. A review of recent works on inclusions. *Mechanics of Materials*, **60**, 144-158.
- Zienkiewicz O.C. and Taylor R.L., 1989. *The Finite Element Methods: Basic Formulation and Linear Problems*, (Vol. 1, 4th Edition), Mc Graw-Hill Book Company, Oxford, 110-147.